

**THE POTENTIAL EFFECTS OF GLOBAL CLIMATE CHANGE
ON THE UNITED STATES:**

APPENDIX A - WATER RESOURCES

Editors: Joel B. Smith and Dennis A. Tirpak

**OFFICE OF POLICY, PLANNING AND EVALUATION
U.S. ENVIRONMENTAL PROTECTION AGENCY
WASHINGTON, DC 20460**

MAY 1989

Text Printed on Recycled Paper

**POTENTIAL CLIMATE CHANGES TO THE
LAKE MICHIGAN THERMAL STRUCTURE**

by

**Michael J. McCormick
NOAA/GLERL
2205 Commonwealth Blvd.
Ann Arbor, MI 48105**

Interagency Agreement No. DW13932957-01-0

CONTENTS

	<u>Page</u>
FINDINGS	6-1
CHAPTER 1: INTRODUCTION	6-2
CHAPTER 2: METHODS	6-4
The Mixed Layer Model	6-4
Model Development	6-4
The Scenarios	6-7
CHAPTER 3: RESULTS	6-8
Base Climatology Simulation	6-8
Impacts of Climate Change	6-11
CHAPTER 4: DISCUSSION, CONCLUSIONS, AND SPECULATIONS	6-23
Interpretation of Results	6-23
Speculations	6-24
REFERENCES	6-25

FINDINGS¹

A one-dimensional numerical model after Garwood (1977) was used to estimate the vertical climatological temperature structure in Lake Michigan. The climatology was based on the model output from simulations of the 1981-1984 offshore temperature field. Quasi-two-dimensional effects were also accounted for by the model by prescribing a weak upwelling velocity during the winter months. Once the climatology was estimated, several different global circulation model (GCM) scenarios were examined. Three different GCM scenarios of doubled CO₂ (2xCO₂) and one transient scenario were simulated. They were (1) Goddard Institute of Space Sciences (GISS) 2xCO₂, (2) the Geophysical Fluid Dynamics Laboratory (GFDL) 2xCO₂ scenario, (3) the Oregon State University (OSU) 2xCO₂ scenario, and (4) GISS Transient scenario A corresponding to the 2010-19 decade (GISS A).

In general, the GISS, GFDL, and OSU simulations suggest the following impact on Lake Michigan. The winter heat content of the lake will be significantly higher than under current climate estimates. The summer heat content will, in general, be higher than the current climate too but not to the same extent as seen during the winter months. The higher winter heat content will cause an earlier setup for thermal stratification by as much as two months and thus a much longer stratified season will result. The earlier onset of stratification coupled with little change in the wind stress pattern will yield stronger stratification. Thus, the greatest differences between the 2xCO₂ and the present climatology are for an earlier, longer duration, and stronger stratification.

The monthly averaged mixed layer depth (mld) may be deeper in the winter and shallower during the summer than current seasonal averages. However, for the winter months this is not true at less than monthly time scales. At higher than monthly frequencies, the present mlds may penetrate to the lake bottom any time during late fall through spring in response to storms and strong surface cooling, while the 2xCO₂ calculated mlds do not. In general, the 2xCO₂-derived mlds are restricted from penetrating deep waters because of the persistence of higher than present water column temperatures (> 4°C), which results in less potential energy being converted into mechanical energy to aid the mixing and deepening process. Thus, the true range in mixed layer depth may well be severely decreased in the future, with only infrequent to rare episodes where the surface mixed layer encroaches on the deep lake bottom, i.e., no turnover. The shallow summer mixed layer will be warmer and more buoyant than presently observed, making it more difficult for entrainment and/or mixing to occur.

The most critical parameter controlling the thermal structure is the wind stress. Calculations of the potential climate impacts were made using uncertain future scenario winds that differ little from the present climate. Should future windspeeds be reduced from those used here, then sensitivity analyses suggest that all of the previously described impacts may underestimate the true impact on the annual thermal cycle.

Simulation results based on the GISS A scenario suggests that some of these effects may be evident 20 to 30 years from now.

¹Although the information in this report has been funded wholly or in part by the U.S. Environmental Protection Agency under Interagency Agreement No. DW13932957-01-0, it does not necessarily reflect the Agency's views, and no official endorsement should be inferred from it.

CHAPTER 1

INTRODUCTION

Lake Michigan is a large lake covering over 57,000 km² with a maximum depth of 281 meters and a mean depth of 85 meters. Because of its large size, the dominant controlling physics of the lake environment is more similar to oceanic situations than it is to "small" lakes. Water temperature is one of the most fundamental physical properties, and accurate knowledge of its distribution is often critical to oceanographic and limnological problems. Despite the importance of temperature, little is known of its climatology in the Great Lakes and in particular that of Lake Michigan. Feit and Goldenberg (1976) determined surface water temperature climatologies for Lakes Superior, Huron, Erie, and Ontario, but the record lengths were short, ranging from only 4 to 10 years. While water intake temperature records of much longer duration exist for many locales in the Great Lakes, their nearshore proximity makes them a poor candidate for constructing meaningful climatologies. Other temperature data sets from more favorable locations exist, but their poor temporal coverage precludes their usage as well.

The most comprehensive data set to date, describing Lake Michigan temperatures in offshore waters, was obtained by the National Data Buoy Center (NDBC) in the central southern basin of the lake from 1981-1984. However, these data too do not fulfill all of the needs for generating a water temperature climatology because of gaps in their temporal coverage and limited spatial coverage as well. In particular, these data only cover the top third of the water column (i.e., 50 meters of the 150-meter mooring depth), and since the mooring is deployed only during the ice-free season, no data exist for the winter months. Consequently, the only alternative is to estimate the climatology by modeling the temperature field, and to use the NDBC data for model testing.

The Garwood (1977) model is used herein to estimate the water temperature climatology for Lake Michigan and potential changes to it that may occur should the climate change. Intermodel comparisons by McCormick and Meadows (1988) and Martin (1985) found the Garwood model to be successful for simulating the seasonal temperature cycle for inland seas and in open ocean applications, respectively. Figure 1 shows the study location and an idealized temperature profile with a shallow surface mixed layer.

The remainder of this report will describe the model development, results, conclusions, and speculations on the Lake Michigan simulations under various future climate scenarios hypothesized by several GCMs.

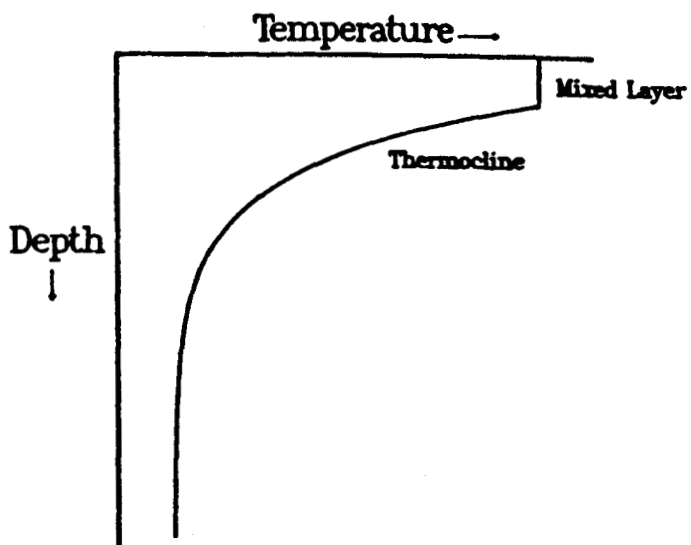
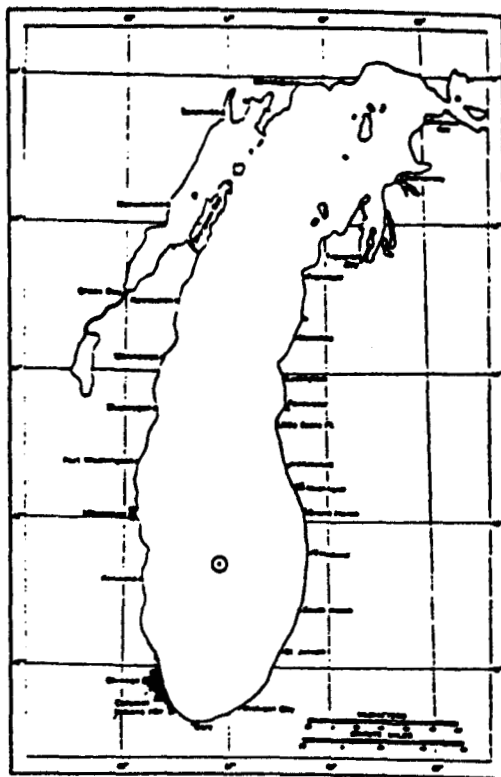


Figure 1. Lake Michigan study location (top) and an idealized temperature profile showing a shallow surface mixed layer (bottom).

McCormick

CHAPTER 2

METHODS

The Mixed Layer Model

The Garwood model version used here is described in McCormick and Meadows (1988). First though, a brief description of the model is in order. The model is one-dimensional in the vertical and is based on the turbulence kinetic energy (TKE) budget. During the summer months, the thermal structure at any given time in general is dependent on the dynamic balance between the wind stress, which tends to destabilize the water column and mix it, and a positive surface heat flux, which warms the surface waters and tends to stabilize the water column and retard mixing. During the winter months when the lake is cooling and the surface heat flux is negative, the wind stress effects on mixing are aided in their efforts by convective mixing, generated from gravitational instabilities due to the surface cooling. These and other important processes are expressed in the TKE equation.

Two of the processes in the TKE budget which also affect the vertical distribution of temperature are viscous dissipation and entrainment due to shear instabilities at the mixed layer base. This version of the Garwood model allows for mixed layer deepening due to turbulent erosion and shear mechanisms. McCormick and Meadows (1988) added the shear instability source to Garwood's model and assumed the major shear source to be from wind-generated pure inertial oscillations. Observations on the frequency distribution of kinetic energy in the Great Lakes support this interpretation (e.g., Saylor et al., 1980; Boyce and Chiochio, 1987). To estimate this contribution to the TKE budget, the shear strength was estimated from one-dimensional momentum equations after Thompson (1976).

If mixed layer deepening is to be realistically described for all possible forcing conditions, then energy dissipation must be explicitly included in the TKE budget. Garwood parameterizes dissipation on two scales. First, energy is removed in proportion to the magnitude of the total TKE, and in the second dissipation process, energy loss is proportional to both the TKE and the depth of the mixed layer. This parameterization of dissipation is advantageous to long-term simulation by avoiding the possible carry-over and buildup of potential energy over annual time scales. Thus, under well-behaved forcing conditions, cyclic solutions are possible.

Model Development

No process-oriented models have been used to do multi-year simulations of temperature in Lake Michigan. Making the transition from seasonal to annual length simulations has been problematic and shortcomings still remain. The time and place chosen for testing and enhancing the Garwood model was 1981-1984 at the site of the NDBC meteorological buoy in the center of the southern basin with a depth of 150 meters. During the ice-free months of 1981-1984, the NDBC hung a thermistor string from their buoy. Nine thermistors were positioned at approximately 5 meters spacing covering the top 50 meters of the water column. Temperatures were recorded at hourly intervals, but the data return and quality were less than ideal. At no time during the 1981-1984 period were all thermistors operational. At various times, as few as two thermistors and as many as seven were recording useful data. Furthermore, analyses of the low frequency response of the data suggests that their accuracy is no better than 0.5°C. Nonetheless, it is the best available data set for this study.

Hourly meteorological data were assembled for a period spanning 30,359 hours from 16 July 1981 through 31 December 1984. (The 16 July date was the date of the first NDBC temperature record.) No offshore water temperature records are available for the 1951-80 period. The meteorological data were obtained from the NDBC buoy and from airport meteorological stations at Milwaukee, Wisconsin, and Muskegon, Michigan. The airport data were averaged with respect to each other and were used whenever buoy meteorological data were missing. Airport meteorological data were used for December in 1981, for January through March and October through December in 1982, and for 1983 and 1984 January through March and for the month of December. Both the airport windspeeds and directions were adjusted for overwater conditions following Schwab (1983).

Hourly observations of windspeed and direction, air temperature, dew point temperature, and total cloud cover were used to force the model. Data on the shortwave global radiation (290-4000 nm) were unavailable and thus were estimated from an empirical model after Cotton (1979). The NDBC meteorological buoy had no provisions for measuring the dew point temperature, essential for estimating the latent heat flux, so all dew point data were taken from shore-based data and were corrected for over-water conditions after Philips and Irbe (1978). Once the meteorological data were assembled, the model testing and development began.

The Garwood model was forced with hourly meteorological data, and numerically integrated over one-hundred-fifty 1-meter-thick grid points at one-hour time steps. The initial conditions were estimated from the 16 July 1981 data and the solution was marched in time for 30,359 hours to the end of 1984. Simulation of the winter regime revealed the need to reevaluate the model physics.

First, the cold winter temperatures of 1982 drove the surface water temperature to freezing conditions on several days. No facilities are included in the model to properly account for ice formation, buildup, and decay. Therefore, the surface temperature was artificially constrained to always be greater than or equal to zero. The modeled surface heat flux during these episodes was set equal to the surface irradiance only and thus does not represent the true surface heat flux. Fortunately, these episodes were infrequent enough in their occurrence so as to not seriously bias the monthly averaged surface heat flux estimate. Second, Farmer and Carmack (1982) noted the importance of the nonlinear pressure temperature term on the density when temperatures are near the temperature of maximum density. The interaction between pressure and temperature has a strong influence on the mixed layer depth in deep lakes, like Lake Michigan, during the winter months. Hence, in contrast to most mixed layer modeling efforts, it was deemed necessary that pressure effects be explicitly accounted for by the equation of state. The equation of state after Pickett and Herche (1984) was used and is shown here in the following equation,

$$\rho = 999.968 - .00773T_0^2 + .526 \times 10^{-4}T_0^3 + .0492P - .00021PT_0 \quad (1)$$

where, ρ = density (kg/m^3), T_0 = temperature $^{\circ}\text{C}$ ($T-3.98$), and P = pressure (bar).

Simulations of the 1982 Lake Michigan springtime transition to thermal stratification with mixed layer models after Denman (1973), Garwood (1977), McCormick and Scavia (1981), and Thompson (1976) suggested the need for yet additional physics. Each model was premature in its timing of the spring transition. Studies of the velocity profile at several locations in the benthic boundary layer of the southern basin by James Saylor of the Great Lakes Environmental Research Laboratory (GLERL) in Ann Arbor, Michigan, has revealed the presence of an Ekman boundary layer. Mass balance calculations suggest that significant upwelling velocities, W_e , (due to a convergence of the Ekman boundary layer) should persist during the winter months in the region where this study was made, and thus it may be an important source/sink of heat to surface waters which must be accounted for by the mixed layer model. The steady-state Ekman pumping velocity, W_e , is given as

$$W_e = (\rho f)^{-1} \text{Curl}(\tau_b) \quad (2)$$

where, f = Coriolis force and τ_b = bottom stress vector. The Curl of the bottom stress vector was estimated from current meter data from four moorings surrounding the central portion of the southern basin. This final model modification was implemented by prescribing W_e for January through May of each year. Constant monthly values were used with a peak velocity of 1 m/day used for March. The monthly velocities are listed in Table 1. The upwelling details will be described in a forthcoming paper.

Specifically, the heat flux due to upwelling, when it occurs, is handled at each time step by first calculating the temperature profile without any consideration of upwelling. Then the temperature change, ΔT_i , at level i , is calculated by equation (3),

$$\Delta T_i = (T_{i+1} - T_i)W_e \Delta t / \Delta Z \quad (3)$$

where, Δt is the time step and ΔZ is the grid size. Equation (3) is applied from the surface ($i=1$) to near bottom ($i=n-1$). Thus, when surface waters are colder/warmer than those at depth, the upwelling heat flux is positive/negative. Although this is a coarse approximation of the true upwelling structure, it nonetheless has

TABLE 1. Model Inputs

WIND SPEED (m/s) (2xCO ₂ - GCM Control)												
Model	Jan	Feb	Mar	Apr	May	Jun	Jul	Aug	Sep	Oct	Nov	Dec
(1)	-.4	-0.5	-1.7	-0.6	-0.8	-0.3	-0.1	0.0	0.1	1.0	1.1	-1.2
(2)	-.3	-1.0	0.3	-0.4	-1.6	-1.6	1.6	0.9	-0.7	-0.6	-0.1	-0.7
(3)	-.5	-0.3	0.3	0.4	-0.2	-0.2	-0.6	0.2	-0.3	-0.4	-0.1	-0.1
(4)	-.1	-0.2	1.0	-0.4	0.1	-0.5	0.1	1.0	0.6	0.1	-0.2	0.1

OVER-WATER AIR TEMPERATURE (°C) (GCM - Base Climatology)												
Model	Jan	Feb	Mar	Apr	May	Jun	Jul	Aug	Sep	Oct	Nov	Dec
(1)	8	8	6	5	3	3	2	3	6	4	7	8
(2)	7	7	6	5	4	8	9	5	6	6	7	8
(3)	6	4	3	3	3	3	3	3	2	3	3	3
(4)	3	3	0	3	0	0	0	0	0	0	0	3

HUMIDITY RATIOS (2xCO ₂ /GCM Control)												
Model	Jan	Feb	Mar	Apr	May	Jun	Jul	Aug	Sep	Oct	Nov	Dec
(1)	1.82	1.49	1.64	1.40	1.30	1.28	1.07	1.28	1.39	1.23	1.54	1.50
(2)	1.56	1.44	1.43	1.37	1.25	1.18	0.97	1.16	1.12	1.31	1.56	1.58
(3)	1.13	1.06	1.05	1.04	1.12	1.17	1.11	1.18	1.25	1.18	1.09	1.14
(4)	1.16	1.20	1.13	1.17	1.06	1.09	1.13	1.14	1.09	1.01	1.05	1.29

SHORTWAVE SOLAR RADIATION RATIOS (2xCO ₂ /GCM Control)												
Model	Jan	Feb	Mar	Apr	May	Jun	Jul	Aug	Sep	Oct	Nov	Dec
(1)	0.92	1.04	0.98	1.03	1.00	0.99	0.98	1.04	1.04	1.12	1.03	0.99
(2)	2.05	1.15	1.15	0.93	1.05	1.05	1.02	1.01	1.01	1.01	1.07	1.74
(3)	1.05	1.04	1.07	1.09	1.03	0.99	1.01	0.98	1.00	1.02	1.00	1.01
(4)	0.97	0.90	1.01	1.01	0.99	0.96	0.93	0.97	1.01	0.99	1.03	0.86

FRACTIONAL CLOUD COVER RATIOS (2xCO ₂ /GCM Control)												
Model	Jan	Feb	Mar	Apr	May	Jun	Jul	Aug	Sep	Oct	Nov	Dec
(1)	1.03	0.93	.97	0.98	1.07	1.09	1.08	1.00	1.06	0.85	1.00	0.93
(2)	1.13	1.18	.92	1.09	0.90	0.83	0.95	0.82	0.90	1.00	1.09	0.92
(3)	0.76	0.83	.74	0.61	0.68	0.94	0.85	1.17	0.83	0.81	0.90	0.91
(4)	1.00	1.05	.97	1.04	0.98	1.19	1.44	1.11	0.92	1.04	1.05	1.03

UPWELLING VELOCITY (m/day) (For All Simulations)						
Jan	Feb	Mar	Apr	May	June through December	
0.2	.55	1.0	.45	0.3	0.	

Model (1) - GISS 2xCO₂
 Model (2) - GFDL 2xCO₂
 Model (3) - OSU 2xCO₂
 Model (4) - GISS A (Transcient Scenario for 2010-19)

enabled more accurate simulation of the upper water column thermal structure when tested over short time periods. An ongoing effort to understand the offshore upwelling structure is presently being addressed at GLERL using a three-dimensional circulation model.

The remaining processes are included in the local heat budget: sensible, latent, net longwave, and shortwave global radiation. The sensible and latent heat fluxes are calculated after bulk aerodynamic formulas with atmospheric stability-dependent exchange coefficients. The stability dependence is based on the work of Businger et al. (1971), and the program is documented in Schwab et al. (1981). The net longwave radiation is calculated after Wyrski (1965), and the penetrating components of the solar irradiance are approximated after Ivanoff (1977). The extinction coefficients for the visible and infrared radiation bands were 0.21 m⁻¹ and 2.85 m⁻¹, respectively.

The Scenarios

Three different GCM results and one transient result were used and compared against the Base climatology, as estimated by the previously described simulation. The three GCM simulations, corresponding to a climate with an effective doubling of atmospheric CO₂ concentration, were made with the following models: (1) GISS, (2) GFDL, and (3) OSU. The transient run was made using a decadal average corresponding to 2010-19 with scenario A. This run is identified in the tables and figures as GISS A.

The 2xCO₂ meteorology used to drive the Lake Michigan simulations was estimated from model output from the 1xCO₂ and 2xCO₂ GCM simulations. These data were formed into a (2xCO₂/1xCO₂) ratio and then used to adjust the Base climatology as described below. The 1xCO₂ GCM simulations were run for a 30-year period corresponding to 1951-1980. The 2xCO₂ general circulation model simulations were also done for a 30-year period, but with a doubling of the atmospheric concentration of CO₂ and other greenhouse gases. Monthly averages were formed for each meteorological parameter, at each grid point, for each simulation. A 2xCO₂/1xCO₂ ratio for each parameter was formed by dividing the monthly averaged quantity from the 2xCO₂ simulation by the 1xCO₂ one. The transient (GISS A) simulation was handled in the same manner. The GCM model output from the grid point closest to central southern Lake Michigan was used to represent the future climate inputs for Lake Michigan. Five different parameters were used from the GCM output: (1) windspeed, (2) air temperature, (3) humidity, (4) incident solar radiation at ground level, and (5) fractional cloud cover. The hourly base meteorological data from 1981 to 1984 were adjusted by multiplication with the applicable (2xCO₂/1xCO₂) GCM ratios. The GCM ratios were held constant on monthly time scales.

The windspeed adjustments were made differently. The supplied GCM monthly windspeed estimates were made by vector averaging rather than by scalar averaging the GCM winds. Thus, when the 2xCO₂/1xCO₂ GCM wind ratios were formed, the calculated ratios were often very large. If the Base climatology winds were multiplied with these ratios, then hurricane force winds would have occurred for at least 2 months out of every simulation year. Therefore, to avoid potentially disastrous results and yet still salvage some of the information in the GCM winds, the differences between the monthly averaged 2xCO₂ and 1xCO₂ windspeeds were used in place of their ratio. These differences were then added to the Base climatology winds. The resulting changes to the wind stress in the Base meteorology were small and more consistent with expectations from other studies (Cohen, 1986). The monthly averaged GCM inputs are shown in Table 1.

McCormick

CHAPTER 3

RESULTS

Base Climatology Simulation

McCormick and Meadows (1988) simulation of Lake Erie temperatures with the Garwood model found the optimal model constants to be identical to those found by Martin (1985) in his simulation of North Pacific Ocean data. The success of this model in such diverse environments instills confidence in the model parameterizations of the governing physics. Thus, all of the model simulations for the Base and future climate scenarios were made without altering the model coefficients.

The Base climatology simulations are shown against surface water temperature data in Figures 2 and 3. The surface temperatures are illustrated for the entire time periods for which the NDBC data were available. For clarity, less than 5% of the approximately 19,000 observations are depicted in the figures.

The lack of time series data throughout the water column and winter temperature data limits the ability to fully evaluate model performance. Nonetheless, from Figures 2 and 3 some of the effects of offshore upwelling and model sensitivity to windspeed are made clear. In Figure 2, low-pass filtered surface temperatures generated by the mixed layer model with no upwelling (i.e., 0.0 meter/day) are shown against data. The effects of a 10% decrease (top of Figure 2) and 10% increase (bottom of Figure 2) in windspeed (WS) are shown as well. The rms error for the 0.0-meter/day simulation was over 4°C for surface temperatures. It is evident that much of this error is contributed by the poor simulation of the 1982 data.

Significant improvement in the surface temperature simulation was made by using a weak upwelling velocity (i.e., "Variable Upwelling" in Figure 3), which was held constant on monthly time scales and operational from January through May (Table 1 and Figure 3). The rms error was approximately 3°C overall, with the 1982 data once again being the most difficult to simulate. Additional improvement in the surface temperature simulation was made in the 0.0-meter/day case with a 10% reduction in windspeed. The overall rms error for these simulations was approximately 2°C, with the major difference between this and the other simulations occurring in 1982. The 1981, 1983, and 1984 rms errors were either similar or slightly worse than the 0.0-meter/day or variable upwelling simulations with unaltered winds. The 2°C rms error was half of the error seen in the 0.0-meter/day simulation and better than 1°C in rms error compared to the simulation with upwelling. The improved rms error occurred because of significant improvements in simulating the spring 1982 data. That year was the coldest winter in this study, and the reduced winds compensated for model shortcomings by reducing lake heat losses during the winter and thus enabled better agreement between model and data during the spring transition period.

If the objective were to solely fit surface temperature data, then the representative choice for our Base climatology would have been obvious. However, there is no physical justification for arbitrarily reducing the windspeeds. And although the rms errors with variable upwelling were larger than the 0.0-m/day case with reduced winds, there is mounting evidence, as described earlier, to justify the use and necessity of upwelling to properly describe the offshore heat budget. Therefore, the simulation with variable upwelling was judged to be the most representative of the region under study and consequently became the "Base" climatology referred to throughout this work.

Again it is important to note here that in terms of surface water temperature simulation of the effects of the "no upwelling" versus the "variable upwelling" cases, either one could be made to mimic the other by adding either a positive or negative 10% bias to the windspeed data. This illustrates that the windspeed is most critical for accurate determination of the Base climatology, and for estimating any possible future alterations to it as well.

Surface Water Temp vs Time

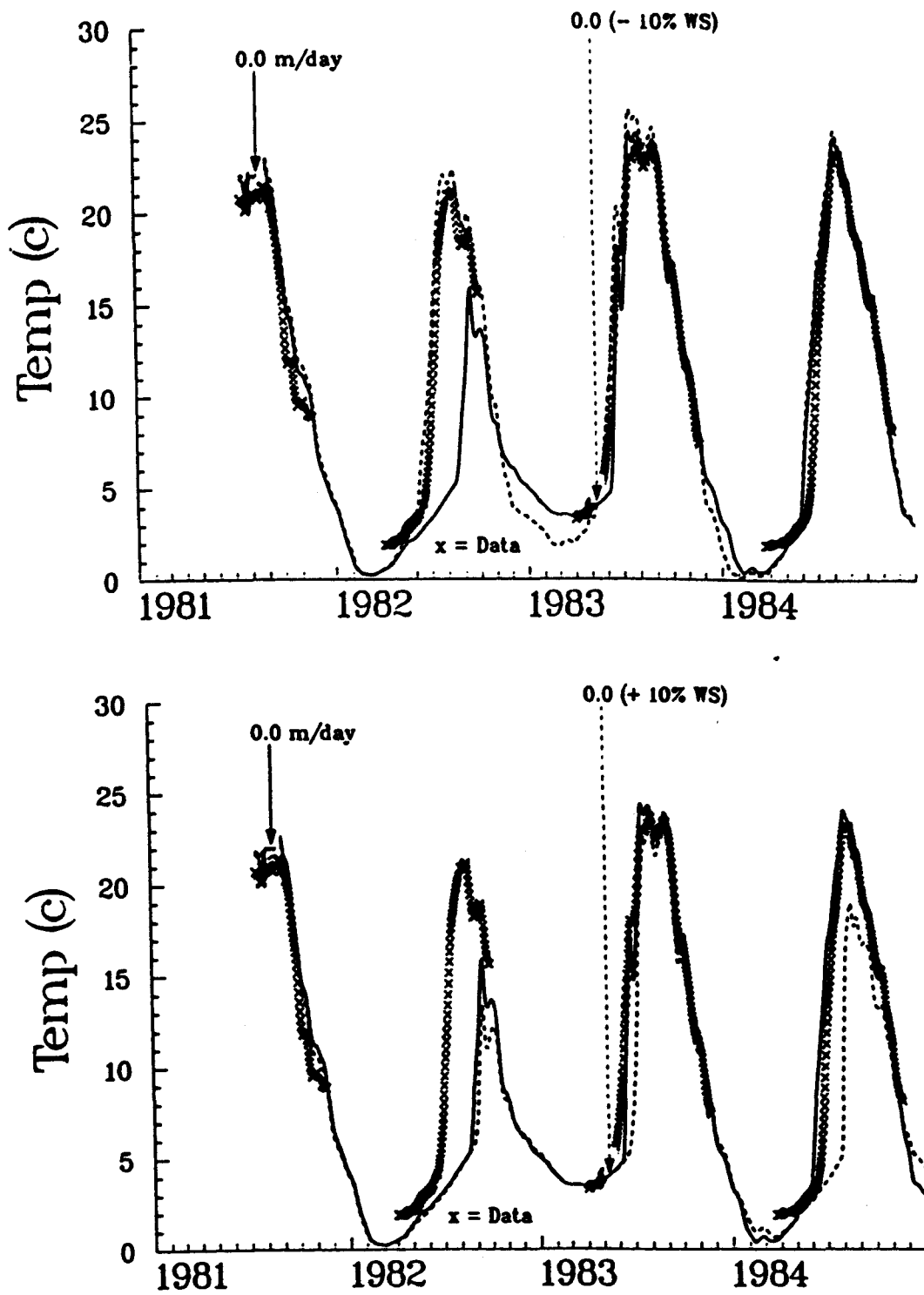


Figure 2. Low-pass filtered (336-hr cutoff) surface temperatures with no upwelling and under different wind conditions. Each curve pattern is duplicated by the line joining it to its label.

Surface Water Temp vs Time

McCormick

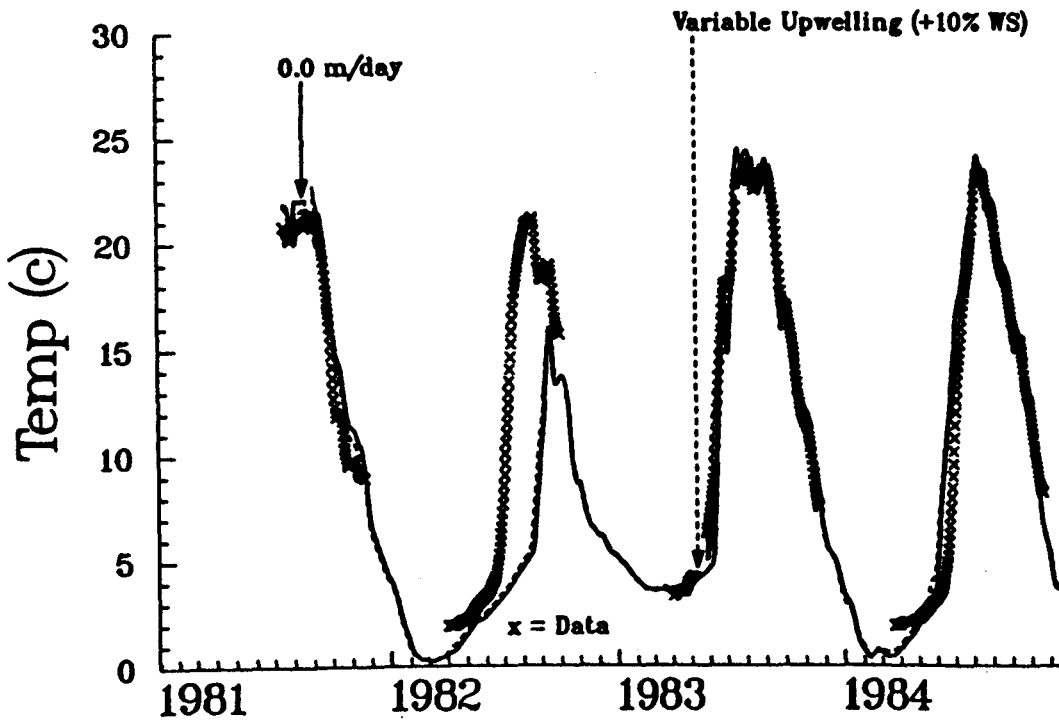
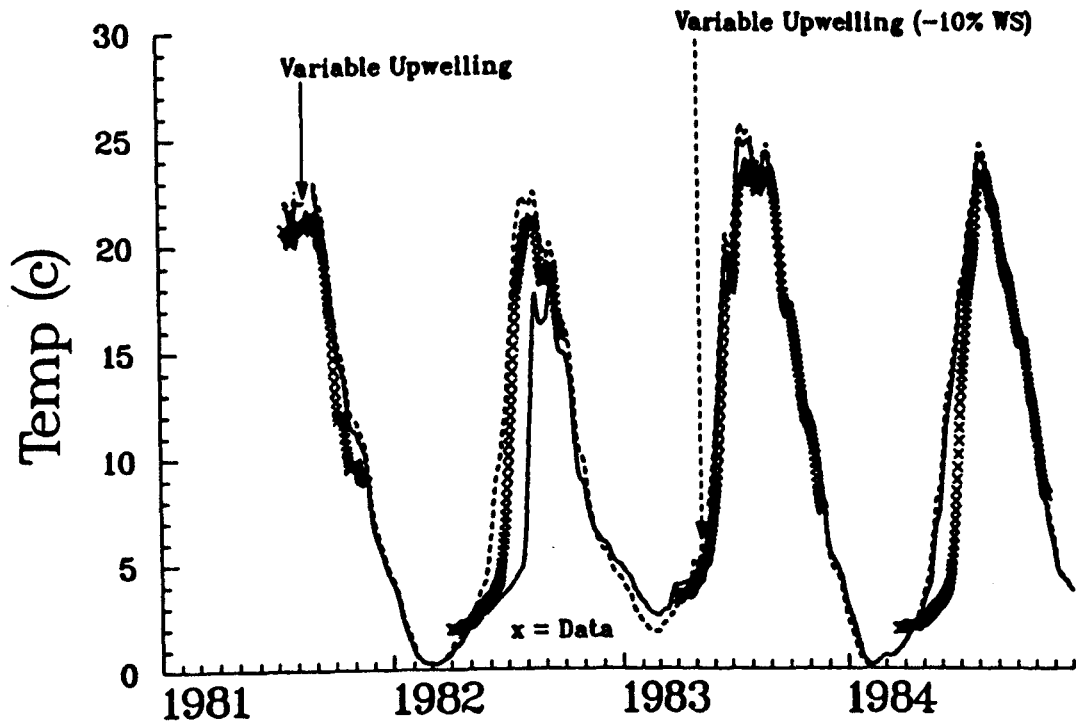


Figure 3. Low-pass filtered (336-hr cutoff) surface temperatures with variable upwelling and under different wind conditions. Each curve pattern is duplicated by the line joining it to its label.

Impacts of Climate Change

Table 2 and Figures 4-11 summarize the model results. Each figure shows the full simulation and its yearly average. Each figure has also been low-pass filtered to better identify possible trends.

Figures 4 and 5 show the net surface heat flux as calculated by the various model simulations. These plots have been low-pass filtered with a 720-hour cutoff period. When upwelling is nonexistent in the simulations (June through December), the net surface heat flux is the only source/sink of heat for the water column. An accurate accounting of the change in heat content from January to June, however, requires that the upwelling heat flux be included in the budget. Table 2 shows monthly estimates of this term, and it should be noted that the method used to estimate it, for Table 2, is subject to error since it involves multiplication of small differences between large numbers.

Two points are of interest in these figures. First, the close similarity between the surface heat fluxes throughout much of the year, particularly during late summer and early fall. And second, the very large heat losses seen in December and January of the first and third winters in the Base simulation (top of Figures 4 and 5). The monthly averaged heat flux components are listed in Table 2 and are discussed below.

Of the five heat flux components, the net longwave and shortwave global radiation terms appear to be the most consistent in their phase and magnitude from model to model (Table 2). The remaining three processes, sensible, latent, and upwelling, show less model to model agreement. The sensible heat flux loss is greatest during January for each model except OSU, where it occurs during December. The latent heat loss reaches its maximum during January for Base and GISS A, while it occurs significantly earlier in the other three models, i.e., October for GISS, September for GFDL, and November for OSU. The averaged upwelling flux shows large model to model differences. In the Base simulation, the upwelling flux, in general, represents a heat source, while in GISS, GFDL, and OSU it is a heat sink. Only in GISS A is the upwelling term positive when averaged over the 5-month period in which it is operational. However, when all the flux terms are summed the net heating rate that results suggests that the annual averaged net heat flux is within 10 W/m² of being zero for all cases. More importantly, the maximum difference between the annual net heat flux under a GCM scenario and Base is only 8 W/m². This emphasizes how the persistence of small changes in the net heat flux can lead to dramatic changes to the environment, and because of the uncertainties surrounding these estimates, why they often lead to controversy.

Figures 6 and 7 show the low-pass filtered surface water temperature. In Figure 6 the Base, GISS, GFDL, and OSU climatologies are shown. These GCM results suggest higher surface temperatures throughout the year. Comparison of the transient scenario for 2010-19 (Figure 7) suggests that higher surface temperatures will prevail from January through July. During the remainder of the year, there is little difference in temperature between GISS A and Base.

As we proceed down in the water column we can begin to estimate more and more of the potential climate impact on Lake Michigan. The mixed layer depth comparisons (Figures 8 and 9) together with Figures 6 and 7 suggest how the heat content of the upper water column may behave in the future. Under the GCM scenarios the mixed layer depth will in general be deeper in the early winter months and will shallow in spring much sooner than in the Base results. This suggests that thermal stratification will begin much earlier than is presently observed. If the interannual variability seen in the top of Figure 8 is truly representative of the Lake Michigan climatology, then the transition to summer stratification under the GCM scenarios may occur two or more months earlier than under the present climate.

This is well illustrated after the first cold winter (Figure 8). In that case, the GCM results (GISS, GFDL, and OSU) suggest that thermal stratification will begin in April rather than the late June date seen in Base. The GISS A results (Figure 9) shows this same tendency but not to the same degree.

TABLE 2. Monthly and annual averaged heat flux components from the Base climatology and GCM simulations

SENSIBLE HEAT FLUX (W/m ²)													
Model	Jan	Feb	Mar	Apr	May	Jun	Jul	Aug	Sep	Oct	Nov	Dec	Annual
(0)	-231	-80	-54	0	9	-2	-2	-2	-23	-26	-70	-169	-54
(1)	-88	-9	0	6	-10	-16	-8	-4	-1	-15	6	-43	-15
(2)	-117	-25	5	9	-8	-12	19	3	-5	-4	-22	-41	-16
(3)	-79	-42	-20	11	-5	-22	-10	-4	-25	-20	-45	-106	-30
(4)	-152	-33	-73	17	5	-9	-4	-4	-31	-30	-72	-96	-40

LATENT HEAT FLUX (W/m ²)													
Model	Jan	Feb	Mar	Apr	May	Jun	Jul	Aug	Sep	Oct	Nov	Dec	Annual
(0)	-141	-63	-65	-24	0	0	-32	-62	-104	-89	-107	-130	-68
(1)	-86	-56	-32	-23	-11	-16	-56	-80	-124	-136	-91	-90	-66
(2)	-125	-51	-66	-23	-17	-49	-116	-126	-145	-112	-96	-97	-85
(3)	-127	-71	-82	-36	-21	-27	-61	-84	-112	-105	-128	-124	-81
(4)	-126	-49	-69	-14	0	1	-18	-54	-108	-96	-100	-92	-60

NET LONGWAVE RADIATION (W/m ²)													
Model	Jan	Feb	Mar	Apr	May	Jun	Jul	Aug	Sep	Oct	Nov	Dec	Annual
(0)	-81	-62	-61	-48	-41	-53	-32	-40	-55	-60	-64	-72	-55
(1)	-57	-48	-47	-44	-58	-63	-49	-37	-30	-57	-40	-52	-48
(2)	-60	-45	-50	-39	-67	-70	-17	-31	-37	-44	-47	-52	-46
(3)	-72	-65	-66	-61	-70	-73	-57	-36	-59	-64	-64	-67	-62
(4)	-68	-49	-65	-35	-47	-59	-41	-43	-61	-60	-64	-57	-54

SHORTWAVE GLOBAL RADIATION (W/m ²)													
Model	Jan	Feb	Mar	Apr	May	Jun	Jul	Aug	Sep	Oct	Nov	Dec	Annual
(0)	58	86	134	185	212	254	248	218	170	112	70	50	150
(1)	52	102	138	197	205	241	235	226	170	148	72	57	153
(2)	109	91	177	165	252	297	264	247	188	114	71	101	173
(3)	84	116	193	276	292	264	275	198	194	139	82	60	181
(4)	56	75	143	183	217	223	193	200	185	108	70	42	141

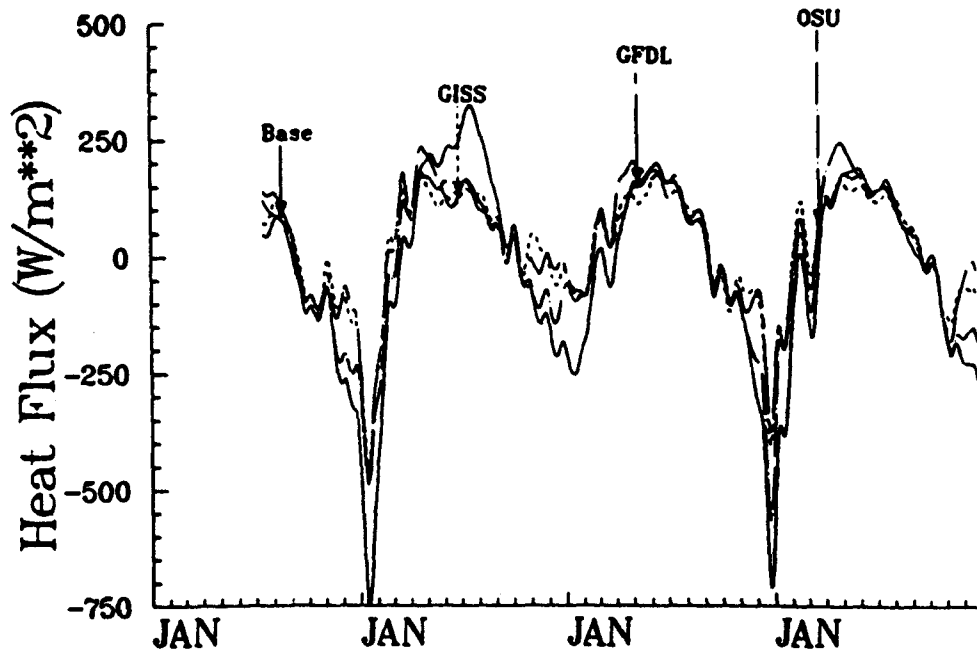
UPWELLING FLUX (W/m ²)													
Model	Jan	Feb	Mar	Apr	May	Jun	Jul	Aug	Sep	Oct	Nov	Dec	Annual
(0)	17	100	128	27	-13	0	0	0	0	0	0	0	21
(1)	-21	-30	-75	-59	-90	0	0	0	0	0	0	0	-22
(2)	-23	-33	-66	-49	-109	0	0	0	0	0	0	0	-23
(3)	-2	9	6	-22	-91	0	0	0	0	0	0	0	-8
(4)	9	41	70	11	-24	0	0	0	0	0	0	0	8

Table 2. (continued)

NET HEATING (W/m ²) (Equals sum of all fluxes)													
Model	Jan	Feb	Mar	Apr	May	Jun	Jul	Aug	Sep	Oct	Nov	Dec	Annual
(0)	-379	-20	83	140	167	199	183	113	-12	-63	-172	-321	-7
(1)	-200	-41	-16	77	36	146	123	105	16	-60	-52	-130	0
(2)	-214	-62	0	64	52	166	151	93	1	-46	-95	-89	1
(3)	-195	-52	31	168	105	142	147	74	-2	-50	-156	-238	-2
(4)	-281	-14	5	163	151	156	130	100	-15	-78	-166	-203	-4

Model (0) - Base Climatology; Models (1)-(4) are the same as in Table 1.

Net Surface Heat Flux vs Time



Averaged Net Surface Heat Flux

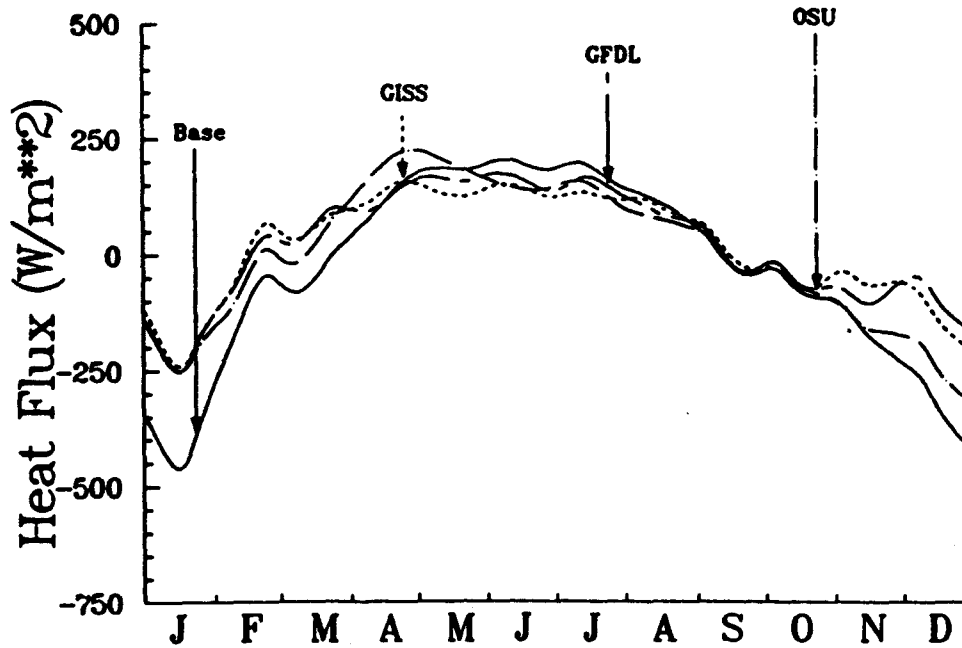
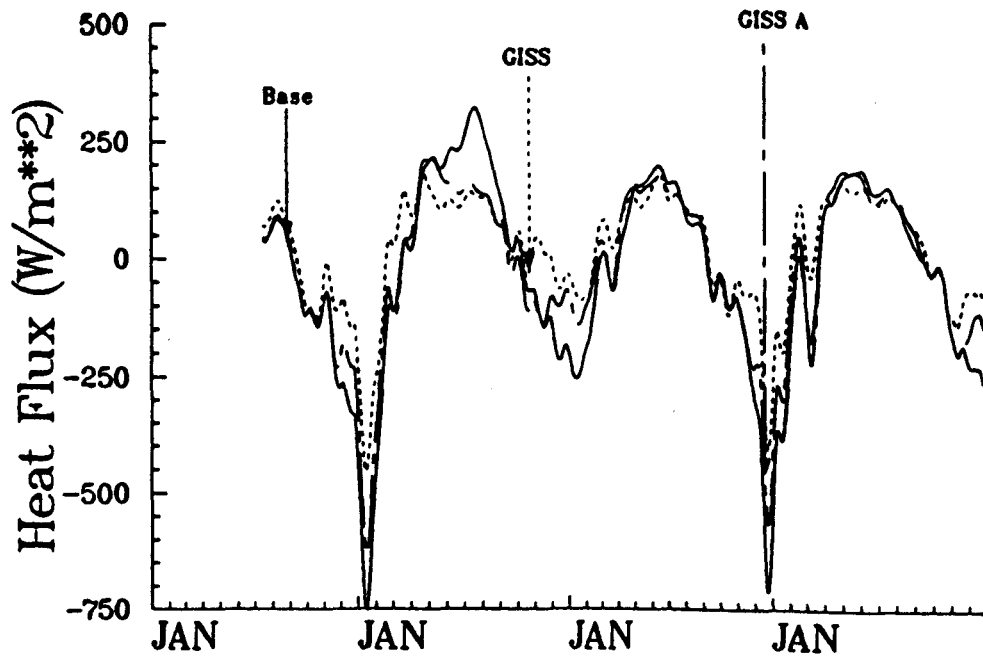


Figure 4. Low-pass filtered (720-hr cutoff) net surface heat flux.

Net Surface Heat Flux vs time

McCormick



Averaged Net Surface Heat Flux

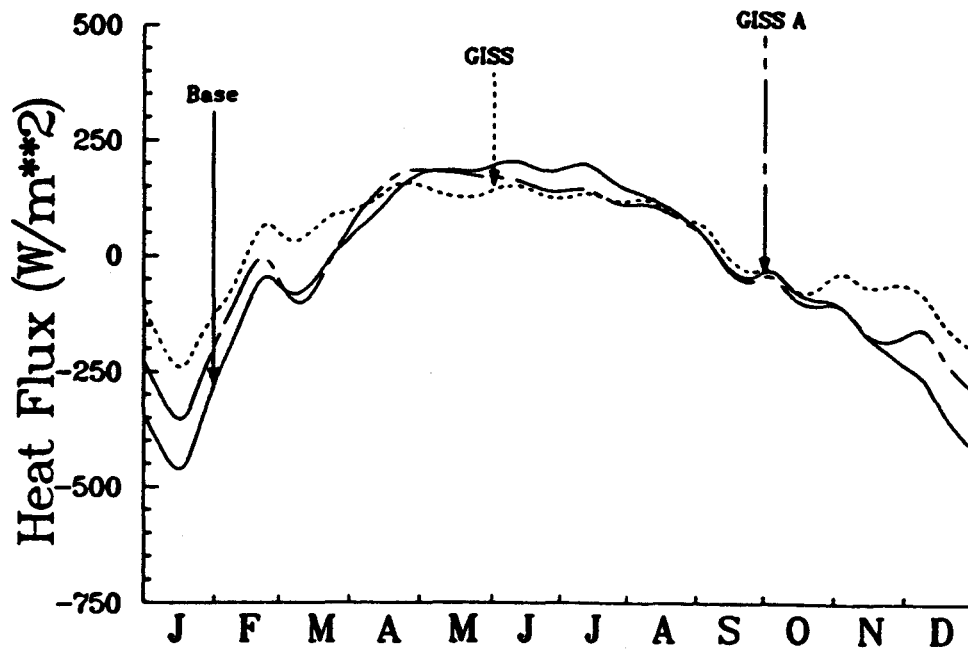
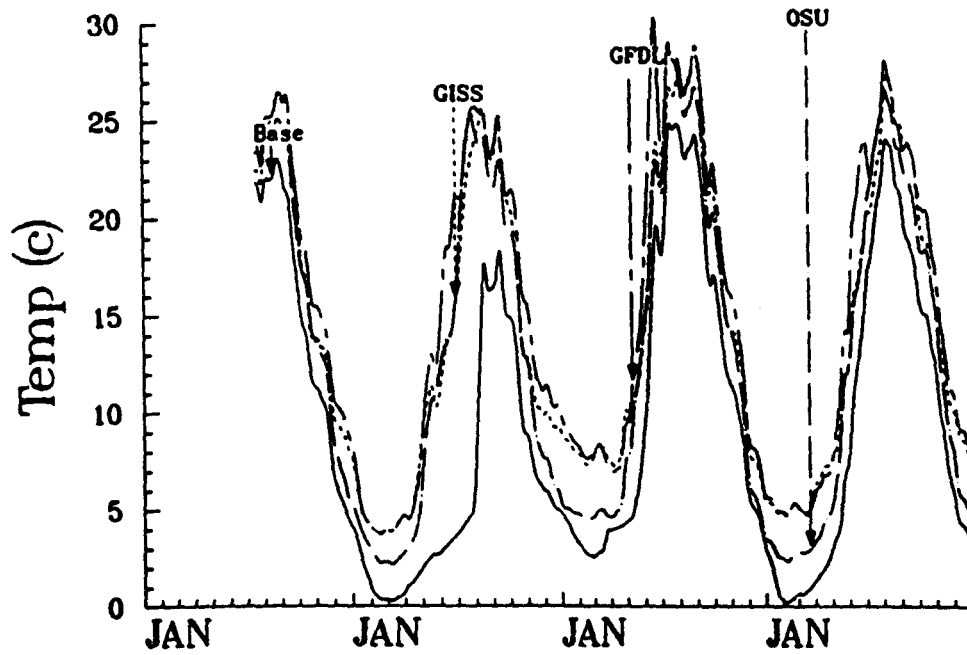


Figure 5. Low-pass filtered (720-hr cutoff) net surface heat flux.

McCormick

Surface Water Temp vs Time



Averaged Surface Water Temp

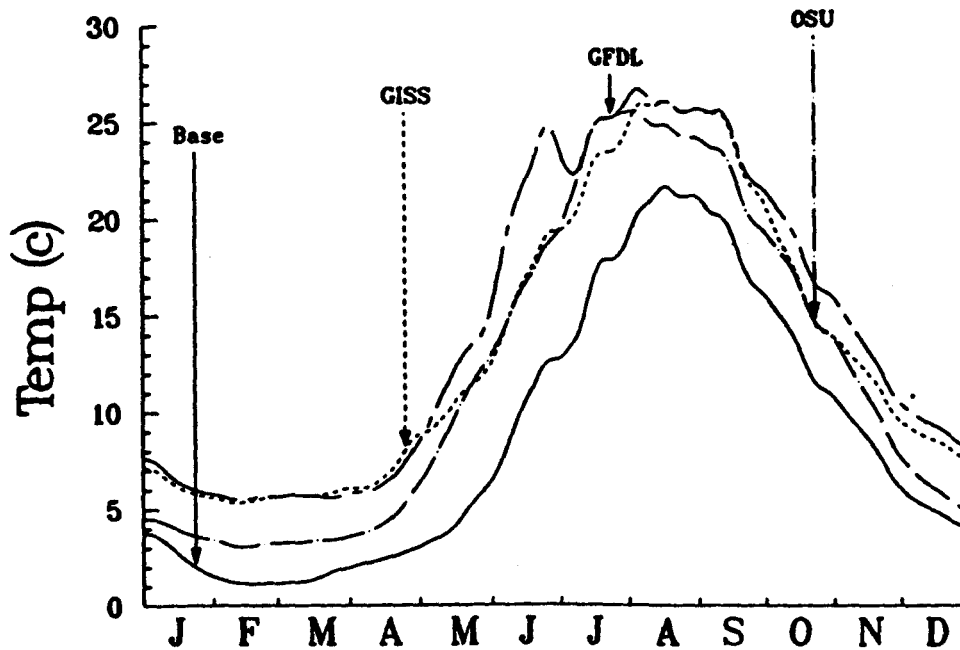
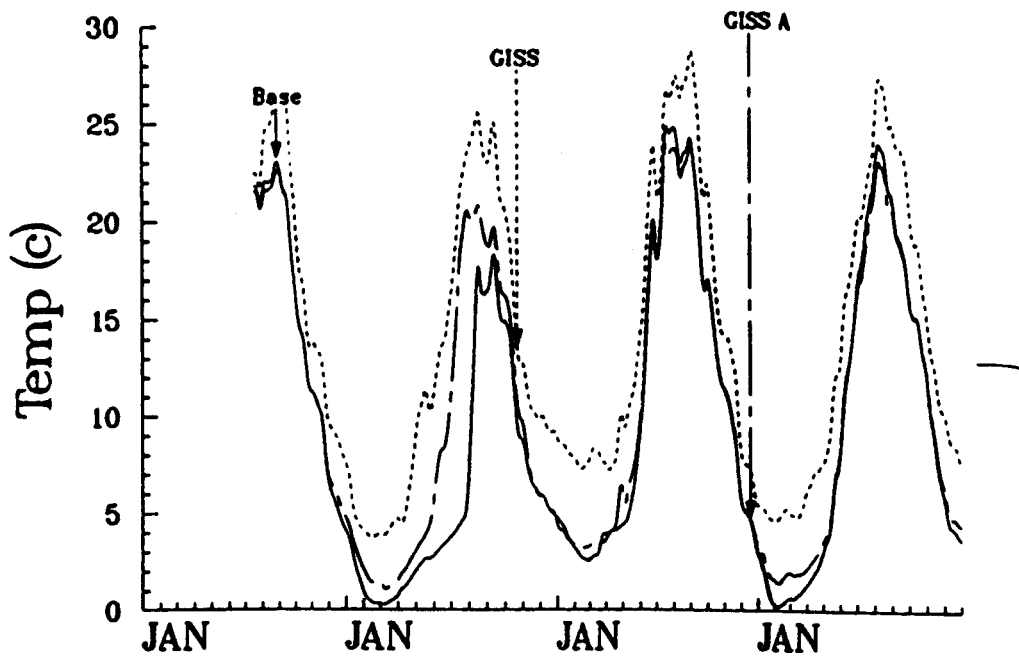


Figure 6. Low-pass filtered (336-hr cutoff) surface water temperature.

Surface Water Temp vs Time

McCormick



Averaged Surface Water Temp

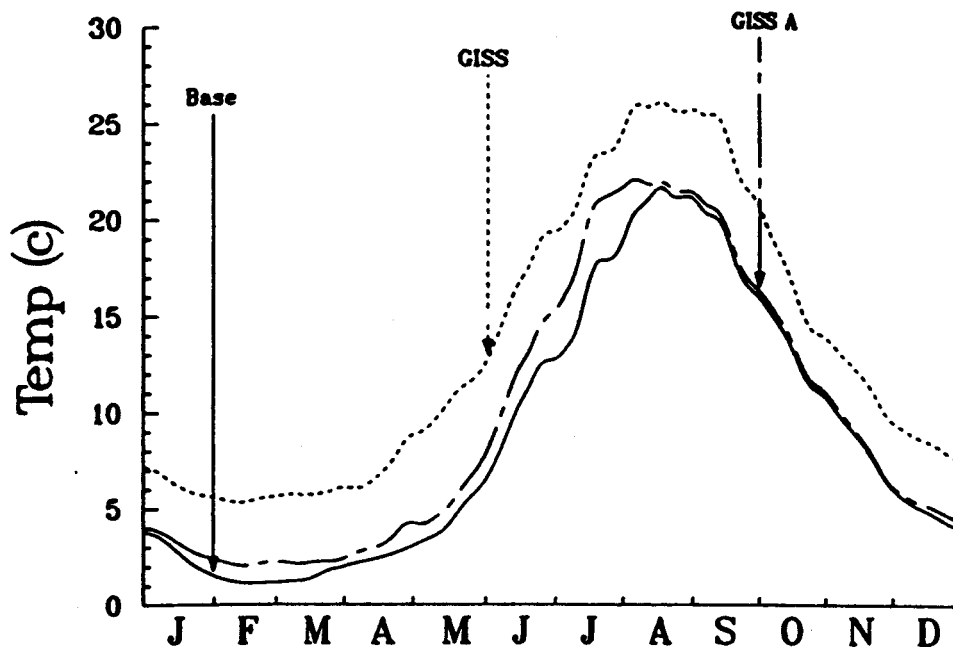


Figure 7. Low-pass filtered (336-hr cutoff) surface water temperature.

McCormick

During the cooling season, the mixed layer depths deepen at approximately the same rate as seen in the current climatology. This reflects the similarity in surface heat content and that changes to the net surface heat flux are smallest during the summer months. Deepening proceeds until late fall when the GCM results suggest an overall cessation of further deepening.

Recall that the simulation is performed for a water column of 150 meter depth. The mixed layer depths in the Base climatology encroach on the bottom for significant periods. Figures 8 and 9 were low-pass filtered with a 720-hour cutoff period; thus mixed layer depth fluctuations with shorter time periods are lost. The mixed layer depths under the GCM scenarios do penetrate to the bottom, on occasion, but not anywhere nearly as often as in the Base simulation.

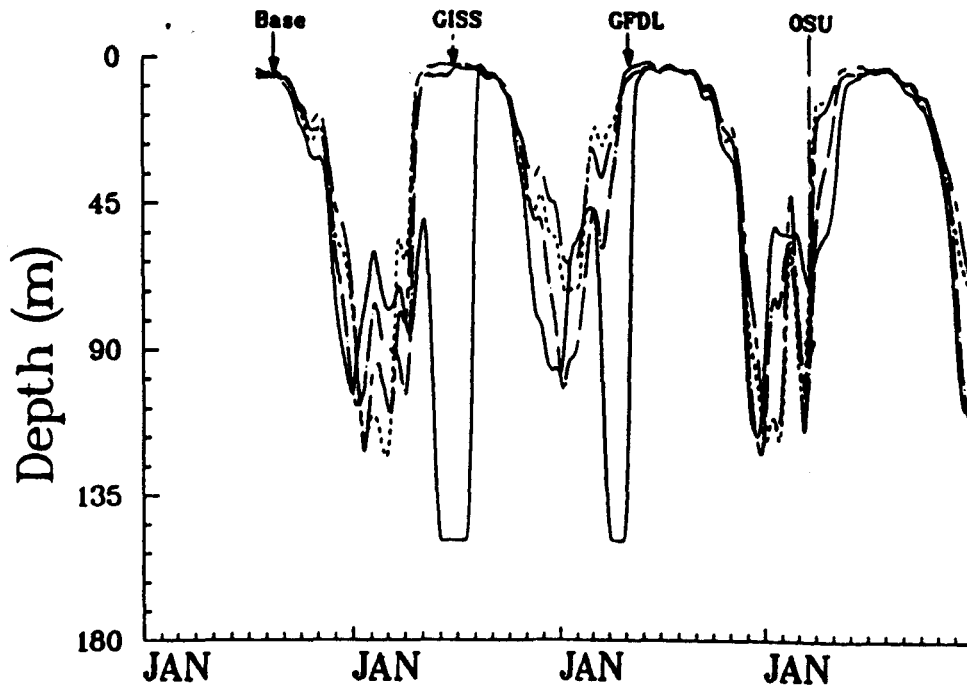
Figures 10 and 11 show potential climate effects on the heat content of the entire water column. This is shown in terms of the vertically averaged water temperature. The GISS and GFDL scenarios show a consistently greater heat content than Base. The biggest differences occur during the winter months when the vertically averaged temperature is significantly higher than that seen in Base. During summer and early fall, however, the heat content increase is less pronounced, with smaller relative increases over the present climatology.

The OSU and GISS A scenarios depart from GISS and GFDL. GISS A (Figure 11) while showing a general warming during the winter and spring, also shows a possible slight decrease in heat storage during the summer months. However, the decreased heat content is small enough to not merit speculation.

The OSU simulation is more similar to the GISS A results than it is to the GFDL and GISS simulations. The OSU run tends to mimic that depicted by GISS A but is displaced to slightly warmer temperatures such that the yearly averaged heat content (Figure 10) shows only zero to positive increases in heat content over Base at all times.

Mixed Layer Depth vs Time

McCormick



Averaged Mixed Layer Depth

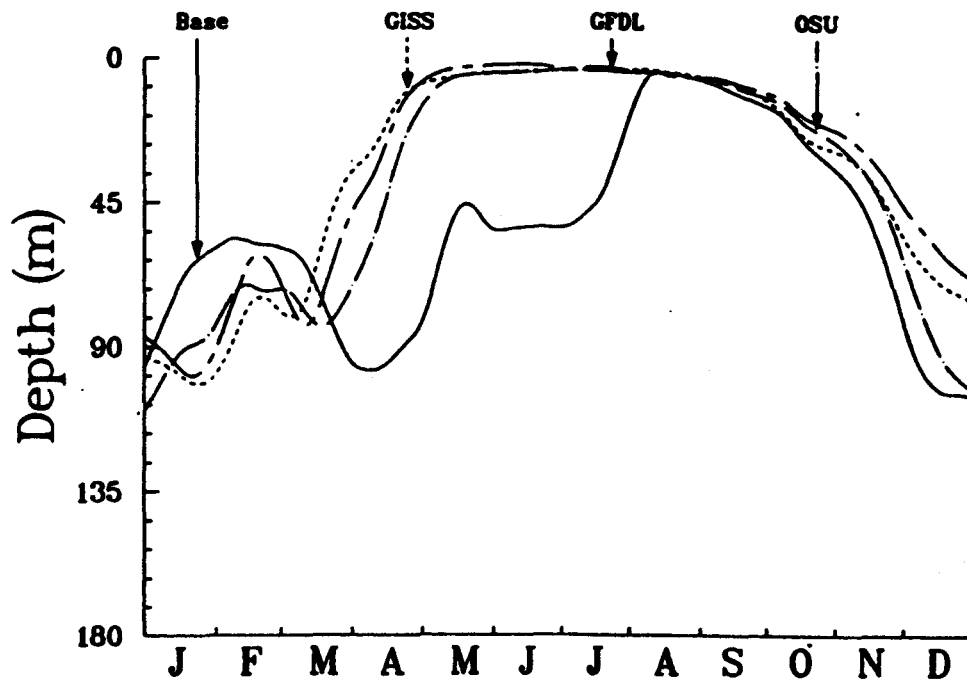
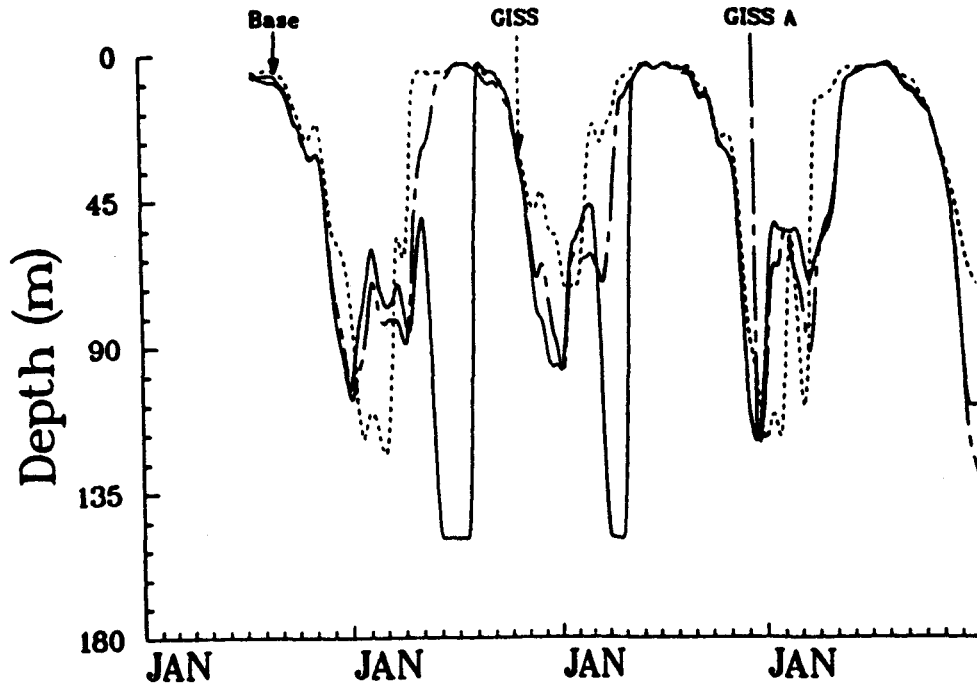


Figure 8. Low-pass filtered (720-hr cutoff) mixed layer depth.

McCormick

Mixed Layer Depth vs Time



Averaged Mixed Layer Depth

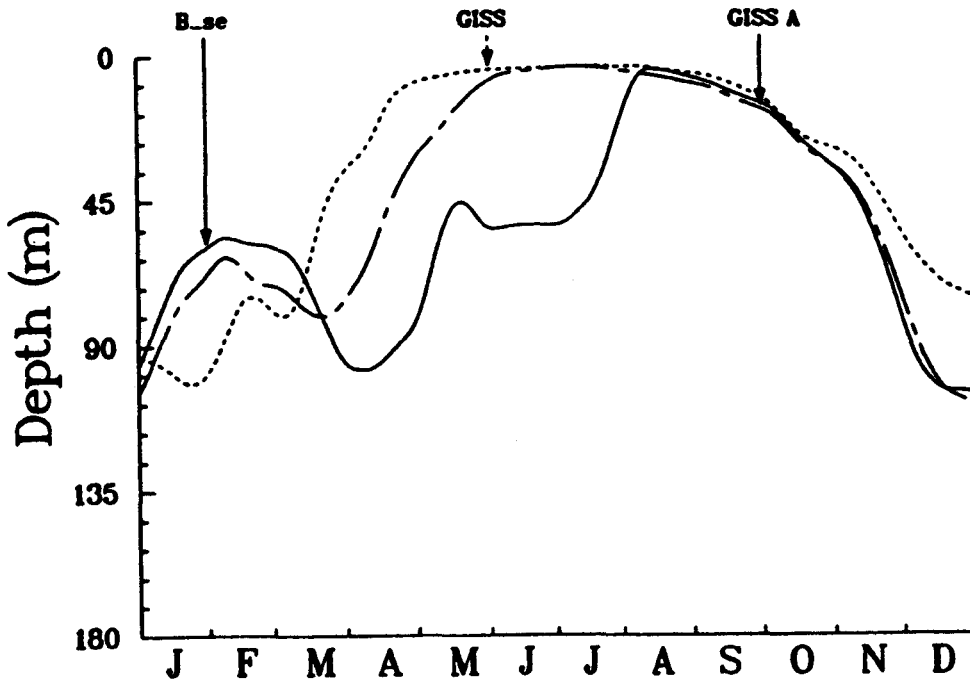
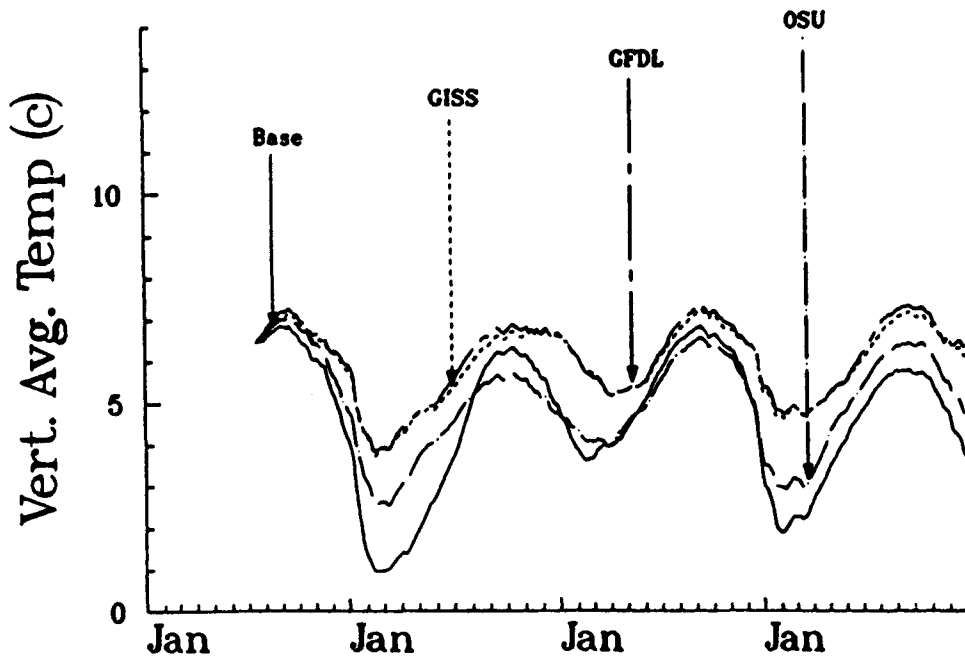


Figure 9. Low-pass filtered (720-hr cutoff) mixed layer depth.

Heat Content vs Time

McCormick



Averaged Heat Content

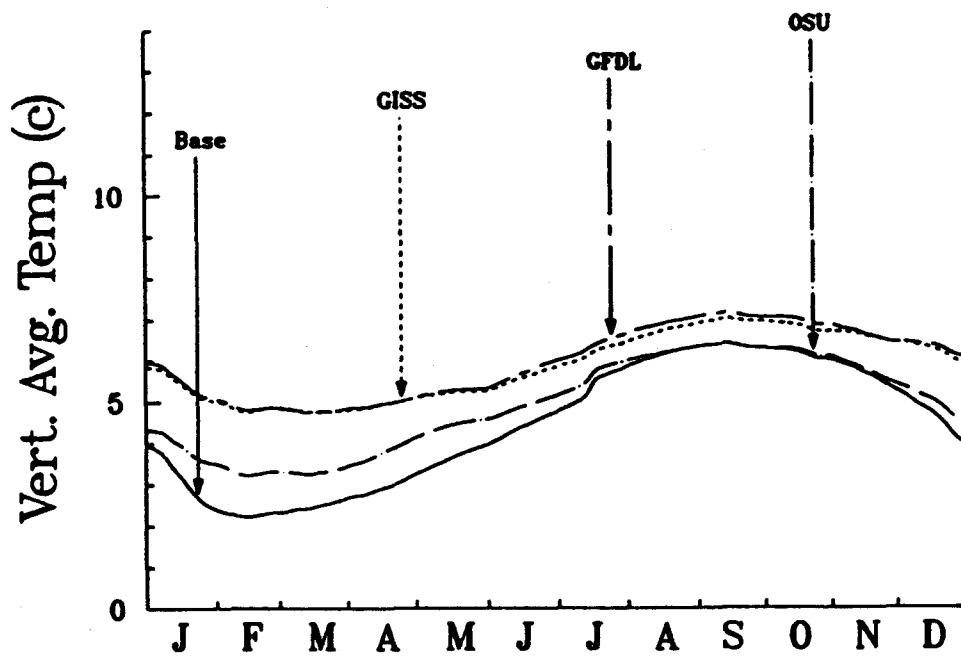
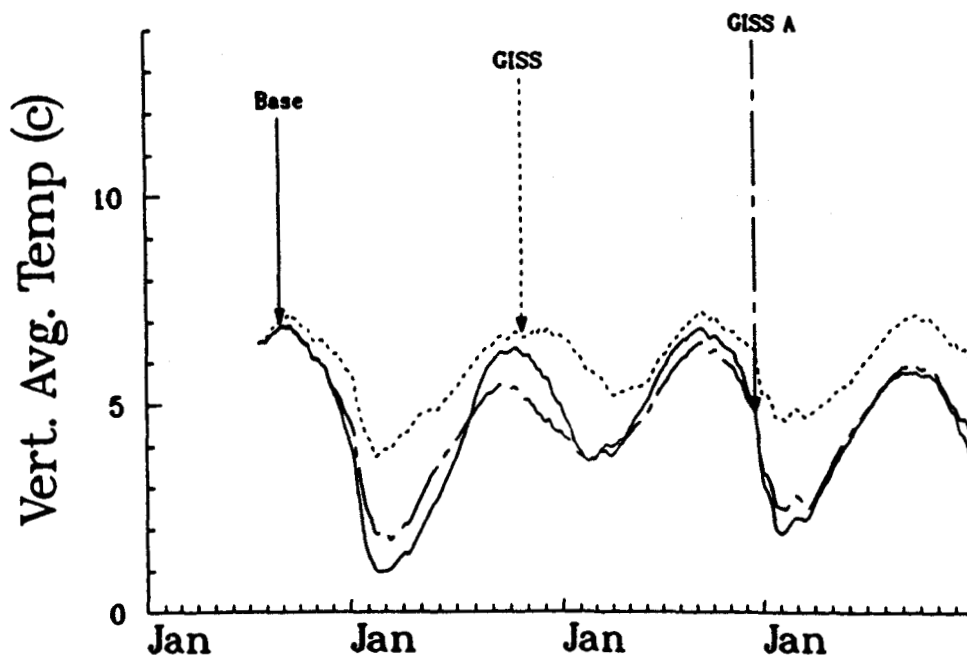


Figure 10. Low-pass filtered (168 hr cutoff) heat content.

Heat Content vs Time



Averaged Heat Content

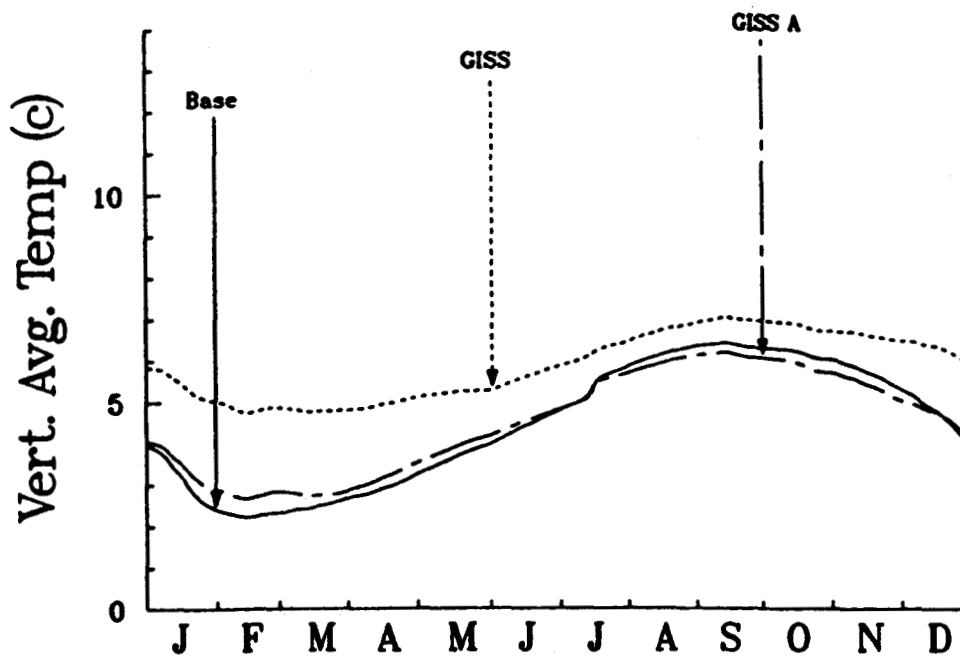


Figure 11. Low-pass filtered (168 hr cutoff) heat content.

CHAPTER 4

DISCUSSION, CONCLUSIONS, AND SPECULATIONS

Interpretation of Results

Tables 1 and 2 suggest that the primary action driving the changes in the GCM simulations is the increased air temperature. Indeed, on a yearly averaged basis the sensible heat flux showed the greatest absolute change from the Base simulation. The large monthly increases in air temperature were up to 8°C (see Table 1) and were responsible for the change in the sensible heat flux. The additional air temperature increase (relative to the GCM output) resulted from over-water modification of the land-based temperature, which was mandated in the Base climatology simulations to avoid excessively large surface heat losses. For consistency purposes, the GCM inputs were treated in an identical fashion.

In general, the GCM results suggest that the mixed layer depth will be shallower than Base. There is one exception to this. In the early winter season (see January and February in Figures 6 and 7), the GCM mixed layer depths are deeper than those in Base, yet still far above the bottom. The reason for the deeper mixed layer during this time period stems from weaker "reverse" stratification in the GCM simulations. In Base, the temperature contrast between surface and bottom waters is much greater than in the GCMs. The strong surface cooling in Base during early winter results in stronger early winter stratification and a shallower surface mixed layer. However, this scene quickly reverses as the lake gains heat. The GCM-simulated mixed layer begins to shallow while the Base generated one deepens. This interesting behavior occurs because of the relationship between the total heat content, as generated by the various simulations, and the temperature of maximum density.

Wind stress has been shown (Adamec and Elsberry, 1984) to be the most sensitive term in controlling thermal structure. For example, in Figure 2 a negative 10% bias in windspeed could cause a 50% improvement in the rms error of surface temperature. In these simulations, however, the wind plays no greater role in the GCM calculations than in the Base simulation. This was supported by comparing the GCM simulations using GCM winds, versus GCM simulations using the Base climatology winds. Differences in the model results were insignificant. However, this by no means suggests that future wind fields are unimportant with respect to present conditions. All it does say is that the monthly vector averaged windspeeds are unimportant and inappropriate for assessing GCM wind sensitivity.

An additional area of concern is the use of monthly averaged data. McCormick and Meadows (1988) have shown that over 90% of the energy associated with mixed layer deepening occurs at daily and higher frequencies. Thus if an accurate assessment of mixing impacts on water quality or other limnological problems is to be made, then the spectral distribution of the wind stress must be well represented. There are numerous examples in the literature where the distribution of physical and chemical tracers is strongly influenced by the frequency and severity of storm events. Therefore, if the physics is to be described through process-oriented models, as used in this study, then the episodic nature of mixing requires high frequency information on all the driving forces, particularly the wind. Although this information was lacking, it does not invalidate this study so much as it points out the need for further study.

Of the heat flux components, the net longwave radiation was the least sensitive to change in the GCM scenarios. This is a consequence more of the empirical formulation used to estimate it than it is a confident estimate of the true response. In fact, there is a growing body of literature suggesting that most empirical longwave radiation formulations are not accurate enough for climatological applications (Frouin et al., 1988; Fung et al., 1984).

The net longwave radiation term is not the only term subject to uncertainty. The surface heat flux can be expected to be in error by as much as 20-30 W/m² on monthly time scales (Wyrski and Urich, 1982). This

McCormick

uncertainty could mask the effects of climate change. The present state of knowledge is too uncertain for quantifying climate change. Yet by using verified, process-oriented models and by referencing the GCM simulations to the Base simulation, the model and data uncertainties are minimized such that greater confidence can be placed on the relative changes. Thus the direction, and not magnitude, of change has been the focus throughout this study.

In conclusion, in each of the GCM scenarios the change is in the direction of significantly higher heat content, particularly during the winter, a deeper mixed layer depth in early winter followed by a shallower one in summer, an earlier onset to density stratification, a longer stratified season, a more buoyant surface mixed layer resulting in less energy available for mixing, and, in general, higher surface water temperatures. The transient scenario suggests that some of these effects may be evident 20-30 years from now.

Speculations

If the GISS or GFDL scenarios are realized, then surface temperatures in offshore waters may never decrease below 4°C. In other words, the lake may not fully overturn during mild winters and thus bottom waters may remain isolated from surface exposure for significant lengths of time. It is possible that the deeper regions of the Great Lakes (i.e., > 100 meters deep) may experience a permanent thermocline with a shallower seasonal one occurring in surface waters, just like much of the world's oceans. In areas where the bottom depths are deep enough for this to occur, and if these regions are polluted, then the reduction in large-scale vertical mixing, as implied by the GCM simulations, may result in anoxic environments being formed where they have never before existed.

Wherever temperature effects are important, impacts will be felt. For example, the earlier warming of surface waters may result in changes to fish recruitment. Undoubtedly, there too must be a reduction in the amount and duration of ice cover. Reducing the ice cover may result in less shoreline protection and increased erosion. And finally, profound changes may occur in the biota through changes in the composition of the food chain to those species which would gain a competitive advantage from changes to the seasonal thermal structure.

REFERENCES

- Adamec, D. and R. L. Elsberry. 1984. Sensitivity of mixed layer predictions at ocean station PAPA to atmospheric forcing parameters. *J. Phys. Oceanogr.* 14:769-780.
- Boyce, F. M. and F. Chiochio. 1987. Inertial frequency oscillations in the central basin of Lake Erie. *J. Great Lakes Res.* 13:542-558.
- Businger, J. A., Wyngaard, J. C., Izumi, Y. and E. F. Bradley. 1971. Flux-profile measurements in the atmospheric surface layer. *J. Atmos. Sci.* 28:181-189.
- Cohen, S. J. 1986. Impacts of CO₂-induced climatic change on water resources in the Great Lakes basin. *Climatic Change.* 8:135-153.
- Cotton, G. F. 1979. ARL models of global solar radiation. p. 165-184. National Climatic Center. In: Hourly solar radiation - surface meteorological observations. Solmet Vol. 2. - Final Report. Dept. of Energy. 184 pp.
- Denman, K. L. 1973. A time-dependent model of the upper ocean. *J. Phys. Oceanogr.* 3:173-184.
- Farmer, D. M. and E. Carmack. 1982. Wind mixing and restratification in a lake near the temperature of maximum density. *J. Phys. Oceanogr.* 11:1516-1533.
- Feit, D. M. and D. S. Goldenberg. 1976. Climatology of surface temperatures of Lakes Superior, Huron, Erie and Ontario. U. S. Dept. of Commerce. NOAA. NWS. TDL Office Note TDL-76-16. Silver Spring, Md. 14 pp.
- Frouin, R., Gautier, C. and J. Morcrette. 1988. Downward longwave irradiance at the ocean surface from satellite data: methodology and in situ validation. *J. Geophys. Res.* 93:597-619.
- Fung, I., Harrison, D. E. and A. A. Lacis. 1984. On the variability of the net longwave radiation at the ocean surface. *Rev. Geophys.* 22:177-193.
- Garwood, R. W., Jr. 1977. An oceanic mixed layer capable of simulating cyclic states. *J. Phys. Oceanogr.* 7:455-468.
- Ivanoff, A. 1977. Oceanic absorption of solar energy. p. 47-72. In: Modelling and prediction of the upper layers of the ocean. E.B. Kraus, ed. New York: Pergamon Press. 325 pp.
- Martin, P. J. 1985. Simulation of the mixed layer at OWS NOVEMBER and PAPA with several models. *J. Geophys. Res.* 90:903-916.
- McCormick, M. J. and D. Scavia. 1981. Calculation of vertical profiles of lake-averaged temperature and diffusivity, in lakes Ontario and Washington. *Water Resour. Res.* 17:305-310.
- McCormick, M. J. and G. A. Meadows. 1988. An intercomparison of four mixed layer models in a shallow inland sea. *J. Geophys. Res.* 93:6774-6788.
- Phillips, D. W. and J. G. Irbe. 1978. Lake to land comparison of wind, temperature and humidity on Lake Ontario during the International Field Year for the Great Lakes (IFYGL). Fisheries and Environment Canada. Atmospheric Environment. CLI-2-77. 51 pp.
- Pickett, R. L. and L. R. Herche. 1984. A simple density equation for Great Lakes Waters. 27th Conf. on Great Lakes Res. St. Catherines, Ontario: Brock University. May 1 - 3.

McCormick

Saylor, J. H., Huang, J. C. K. and R. O. Reid. 1980. Vortex modes in southern Lake Michigan. *J. Phys. Oceanogr.* 10:1814-1823.

Schwab, D. J., Bennett, J. R. and A. T. Jessup. 1981. A two-dimensional lake circulation modeling system. NOAA Tech. Mem. ERL GLERL - 38. Ann Arbor, Mi. 79 pp.

Schwab, D. J. 1983. Numerical simulation of low-frequency current fluctuations in Lake Michigan. *J. Phys. Oceanogr.* 13:2213-2224.

Thompson, R. O. R. Y. 1976. Climatological numerical models of the surface mixed layer of the ocean. *J. Phys. Oceanogr.* 6(4):496-503.

Wyrski, K. 1965. The average annual heat balance of the North Pacific Ocean and its relation to ocean circulation. *J. Phys. Oceanogr.* 18:4547-4559.

Wyrski, K. and L. Urich. 1982. On the accuracy of heat storage computations. *J. Phys. Oceanogr.* 12: 1411 - 1416.